(12) INTERNATIONAL APPLICATION PUBLISHED UNDER THE PATENT COOPERATION TREATY (PCT)

(19) World Intellectual Property Organization
International Bureau

(43) International Publication Date
22 May 2020 (22.05.2020)

WIPO | PCT

(10) International Publication Number
WO 2020/099649 A1

(51) International Patent Classification:
G06T 11/00 (2006.01)

(21) International Application Number:
PCT/EP2019/081515

(22) International Filing Date:
15 November 2019 (15.11.2019)

(25) Filing Language: English

(26) Publication Language: English

(30) Priority Data:
62/768,131 16 November 2018 (16.11.2018) US

(71) Applicant: **KONINKLIJKE PHILIPS N.V.** [NL/NL]; High Tech Campus 52, 5656 AG Eindhoven (NL).

(72) Inventors: **ANDREYEV, Andriy**; High Tech Campus 5, 5656 AE Eindhoven (NL). **SONG, Xiyun**; High Tech Campus 5, 5656 AE Eindhoven (NL). **MANJESHWAR, Ravindra, Mohan**; High Tech Campus 5, 5656 AE Eindhoven (NL).

(74) Agent: **PHILIPS INTELLECTUAL PROPERTY & STANDARDS**; High Tech Campus 5, 5656 AE Eindhoven (NL).

(81) Designated States *(unless otherwise indicated, for every kind of national protection available)*: AE, AG, AL, AM, AO, AT, AU, AZ, BA, BB, BG, BH, BN, BR, BW, BY, BZ, CA, CH, CL, CN, CO, CR, CU, CZ, DE, DJ, DK, DM, DO, DZ, EC, EE, EG, ES, FI, GB, GD, GE, GH, GM, GT, HN, HR, HU, ID, IL, IN, IR, IS, JO, JP, KE, KG, KH, KN, KP, KR, KW, KZ, LA, LC, LK, LR, LS, LU, LY, MA, MD, ME, MG, MK, MN, MW, MX, MY, MZ, NA, NG, NI, NO, NZ, OM, PA, PE, PG, PH, PL, PT, QA, RO, RS, RU, RW, SA, SC, SD, SE, SG, SK, SL, SM, ST, SV, SY, TH, TJ, TM, TN, TR, TT, TZ, UA, UG, US, UZ, VC, VN, ZA, ZM, ZW.

(84) Designated States *(unless otherwise indicated, for every kind of regional protection available)*: ARIPO (BW, GH, GM, KE, LR, LS, MW, MZ, NA, RW, SD, SL, ST, SZ, TZ, UG, ZM, ZW), Eurasian (AM, AZ, BY, KG, KZ, RU, TJ, TM), European (AL, AT, BE, BG, CH, CY, CZ, DE, DK, EE, ES, FI, FR, GB, GR, HR, HU, IE, IS, IT, LT, LU, LV, MC, MK, MT, NL, NO, PL, PT, RO, RS, SE, SI, SK, SM, TR), OAPI (BF, BJ, CF, CG, CI, CM, GA, GN, GQ, GW, KM, ML, MR, NE, SN, TD, TG).

Declarations under Rule 4.17:

— *as to applicant's entitlement to apply for and be granted a patent (Rule 4.17(ii))*

(54) **Title:** EDGE PRESERVING PENALIZED RECONSTRUCTION FOR STEP-AND-SHOOT AND MOTION COMPENSATED POSITRON EMISSION TOMOGRAPHY (PET) STUDIES

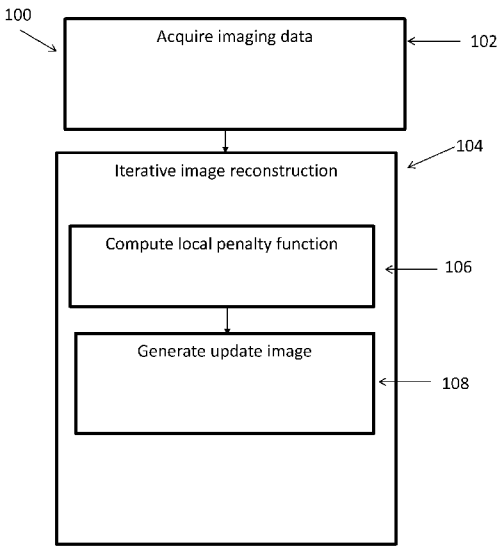

Figure 2

(57) **Abstract:** A non-transitory computer-readable medium stores instructions readable and executable by a workstation (18) including at least one electronic processor (20) to perform an imaging method (100). The method includes: receiving imaging data on a frame by frame basis for frames along an axial direction with neighboring frames overlapping along the axial direction wherein the frames include at least a volume (k) and a succeeding volume (k+1) at least partially overlapping the volume (k) along the axial direction; and generating an image of the volume (k) using an iterative image reconstruction process in which an iteration of the iterative image reconstruction process includes: computing a local penalty function for suppressing noise over the volume (k) including reducing the value of the local penalty function in an overlap region; generating an update image of the volume (k) using imaging data from the volume (k) and further using the local penalty function.

WO 2020/099649 A1

[Continued on next page]

Published:
— *with international search report (Art. 21(3))*

Edge preserving penalized reconstruction for step-and-shoot and motion compensated positron emission tomography (pet) studies

FIELD

[0001] The following relates generally to the medical imaging arts, positron emission tomography (PET) imaging and image reconstruction arts, regularized iterative image reconstruction arts, and related arts.

BACKGROUND

[0002] Image quality in positron emission tomography (PET) is strongly dominated by noise. Iterative maximum-a-posteriori penalized reconstruction (PR) using an edge-preserving or contrast preserving prior is one approach to suppress noise while retaining small features (e.g. tumors) that may be of clinical interest. Some edge-preserving or contrast preserving penalties include: (1) relative difference penalty (RDP) (see, e.g., J. Nuyts et al., "A concave prior penalizing relative differences for maximum-a-posteriori reconstruction in emission tomography," *IEEE Trans. Nucl. Sci.*, 2002); (2) anisotropic diffusion penalty (ADP) (see, e.g., H. Zhu, "Image reconstruction for positron emission tomography using fuzzy nonlinear anisotropic diffusion penalty," Med Bio Eng Comput, 2006), and so on. In most edge-preserving penalties, a tuning parameter establishes sensitivity to the edge transition in the reconstructed images, and imaging data below the sensitivity threshold is smoothed by a strong low-pass filter.

[0003] Commercial PET cameras have a limited axial field of view (FOV) due to the finite axial extent of the PET detector rings or array. Therefore, a "whole body" patient scan is typically acquired in a serial "step-and-shoot" mode at multiple bed positions with certain overlap between the bed positions. For practical reasons, each bed position is typically reconstructed separately without waiting for the PET data for the next bed position to be fully acquired, and the reconstructed individual frame images are knitted into a single whole-body image. Each bed position overlaps to ensure smooth signal transition in the axial direction. Typically, for whole body studies, more than 50% of the scanned axial extent will be covered in overlap slices. Therefore, in every reconstructed image volume, there will be one or two sub-volumes that are covered by the acquired counts from either previous bed position or next bed position (note that, as discussed herein, it is assumed that in all situations considered the number of bed positions is at least larger than one).

[0004] Instead of reconstructing each bed position separately and then knitting the images together in image space, in an alternative approach the counts are pre-combined (either

in sinogram format or list mode) before the reconstruction without overcomplicating the imaging workflow (see, e.g., Z. Sun, et al. "Reconstruction and combination of PET multi-bed image," US Pub. No. 2017/0103551). However, previous work shows that at least Ordered Subset Expectation Maximization (OSEM) iterative image reconstruction algorithm demonstrates quasi-linear behavior and there is little practical benefit of pre-combining the counts before the reconstruction except for ultra-low count studies (see, e.g., S. Ross et al., "A method of overlap correction for fully 3D OSEM reconstruction of PET data", MIC, 2004). In the case of reconstructing every bed position separately, each bed position image can have noisier appearance in the edge slices due to effective "loss" of data at the edges. But, the noise can generally be compensated during the image knitting procedure (i.e., when the individual bed position images are combined into a single whole-body image).

[0005] The following discloses new and improved systems and methods to address these problems.

SUMMARY

[0006] In one disclosed aspect, a non-transitory computer-readable medium stores instructions readable and executable by a workstation including at least one electronic processor to perform an imaging method. The method includes: receiving imaging data on a frame by frame basis for frames along an axial direction with neighboring frames overlapping along the axial direction wherein the frames include at least a volume (k) and a succeeding volume (k+1) at least partially overlapping the volume (k) along the axial direction; and generating an image of the volume (k) using an iterative image reconstruction process in which an iteration of the iterative image reconstruction process includes: computing a local penalty function for suppressing noise over the volume (k) including reducing the value of the local penalty function in an overlap region; generating an update image of the volume (k) using imaging data from the volume (k) and further using the local penalty function.

[0007] In another disclosed aspect, an imaging system includes a positron emission tomography (PET) imaging device. At least one electronic processor is programmed to: receive imaging data on a frame by frame basis for frames along an axial direction with neighboring frames overlapping along the axial direction wherein the frames include at least a volume (k) and a succeeding volume (k+1) at least partially overlapping the volume (k) along the axial direction; and generate an image of the volume (k) using an iterative image reconstruction process in which an iteration of the iterative image reconstruction process includes: computing a local penalty function for suppressing noise over the volume (k)

including reducing the value of the local penalty function in an overlap region, the local penalty function depending on the total coincidence counts passing through the voxel being penalized, and the value of the local penalty function is reduced in the overlap region by an amount compensating for the total coincidence counts passing through the voxel being penalized in the succeeding volume $k + 1$; generating an update image of the volume (k) using imaging data from the volume (k) and further using the local penalty function. The reconstructing includes: combining the number of counts from the volumes (k) in the imaging data into a total volume; and reconstructing the total volume into a reconstructed image.

[0008] In another disclosed aspect, an imaging method performed on imaging data on a frame by frame basis for frames along an axial direction with neighboring frames overlapping along the axial direction wherein the frames include at least a volume (k) and a succeeding volume (k+1) at least partially overlapping the volume (k) along the axial direction includes: generating an image of the volume (k) using an iterative image reconstruction process in which an iteration of the iterative image reconstruction process includes: computing a local penalty function for suppressing noise over the volume (k) including reducing the value of the local penalty function in an overlap region, the local penalty function depends on local geometric sensitivity of the PET imaging device and the value of the local penalty function is reduced in the overlap region by an amount compensating for loss of geometric sensitivity due to axial truncation of the volume (k); generating an update image of the volume (k) using imaging data from the volume (k) and further using the local penalty function. The reconstructing includes reconstructing the volume (k) of the imaging data separately from the other volumes (k) of the imaging data into a reconstructed image.

[0009] In another disclosed aspect, an imaging method performed on imaging device to acquire imaging data on a frame by frame basis for frames along an axial direction with neighboring frames overlapping along the axial direction wherein the frames include at least a volume (k) and a succeeding volume (k+1) at least partially overlapping the volume (k) along the axial direction includes: generating an image of the volume (k) using an iterative image reconstruction process in which an iteration of the iterative image reconstruction process includes: adjusting the imaging data with respiratory gating using two or more gate phases and motion detected in the gate phases; computing a local penalty function for suppressing noise over the volume (k) including reducing the value of the local penalty function in an overlap region; generating an update image of the volume (k) using imaging data from the volume (k) and further using the local penalty function.

[0010] One advantage resides in utilizing all available counts from a PET imaging device to properly adjust parameters of a reconstruction penalty function.

[0011] Another advantage resides in providing an edge-preserving penalized reconstruction process that avoids over-smoothing of a final image, leading to potentially lost image features.

[0012] Another advantage resides in providing an edge-preserving penalized reconstruction process that avoids under-smoothing of a final image, leading to potential noise in the image.

[0013] Another advantage resides in, when data in overlapping regions of imaging data are combined before image reconstruction, reducing a penalty function proportionally to an effective sensitivity increase introduced by combining neighboring images in the overlap region to preserve a spatial resolution of a reconstructed image.

[0014] Another advantage resides in, when data in overlapping regions of imaging data are not combined before image reconstruction, reducing a penalty function to preserve a spatial resolution of a reconstructed image.

[0015] Another advantage resides in scaling a penalty function with an acquisition duration ratio between two imaging frames.

[0016] Another advantage resides in dynamically adjusting penalty parameters of a penalty function with count-end-points-adjusted motion corrected respiratory or cardiac gated or dynamic studies.

[0017] A given embodiment may provide none, one, two, more, or all of the foregoing advantages, and/or may provide other advantages as will become apparent to one of ordinary skill in the art upon reading and understanding the present disclosure.

BRIEF DESCRIPTION OF THE DRAWINGS

[0018] The disclosure may take form in various components and arrangements of components, and in various steps and arrangements of steps. The drawings are only for purposes of illustrating the preferred embodiments and are not to be construed as limiting the disclosure.

[0019] FIGURE 1 diagrammatically shows an imaging system according to one aspect;

[0020] FIGURES 2 and 3 show exemplary flow chart operations of the system of FIGURE 1; and

[0021] FIGURES 4a-c show a comparison of a standard reconstructed image versus an image reconstructed with the flow chart operations of FIGURE 2.

DETAILED DESCRIPTION

[0022] Iterative penalized PET image reconstruction employs an update function that includes a penalty term designed to penalize (i.e. suppress) noise while retaining edges. For example, a relative difference penalty (RDP) employs a penalty $P \propto 1/\gamma$ where the term γ is the edge preservation parameter. Larger values of γ produce a smaller penalty P which enhances preservation of features (i.e., "edges") such as small lesions but also leads to retention of more noise; whereas, smaller values of γ increase the penalty which improves noise suppression, but can also lead to removal of clinically significant structures (i.e., "edges") such as small lesions. In a variant approach, the penalty is locally tuned, for example by using $\gamma = \sqrt{\lambda_i s_i}$ where λ_i is the value of the voxel indexed by i and s_i is the geometric sensitivity at the voxel i which is proportional to the number of lines of response (LORs) passing through the voxel i. This formulation is premised on the expectation that if more LORs pass through the voxel i (hence higher s_i) then there should be more counts in the vicinity and hence noise should be lower at voxel i, so that a smaller penalty P can be used to enhance edges while still suppressing the (relatively low) noise. In an alternative tuning, the geometric sensitivity s_i is replaced by a term which quantifies the total counts in a local neighborhood around voxel i. Again, higher total counts in the local neighborhood tends to correspond with lower noise, so that a lower penalty P can be used.

[0023] It is recognized herein that such penalization frameworks can be less effective in the case of overlap regions of step-and-shoot PET imaging. In the step-and-shoot approach (also known as multi-bed imaging or similar nomenclatures), the patient is stepped through the scanner to image successive axial portions ("bed positions") of the patient. The data acquired at each bed position is thus axially truncated at edge slices corresponding to the locations of the outermost detector rings of the PET scanner at that bed position. Conventionally, the PET counts acquired at each bed position are separately reconstructed (but possibly using information from neighboring bed positions to estimate out-of-FOV scatter), and the resulting bed position images are knitted together at the overlaps by weighted averaging of the voxel values in the overlapping regions of the bed position images. In such an approach, however, the local tuning of the penalty is computed using geometric sensitivities s_i for that bed position. For outer slices of the bed position, sensitivities s_i become small because the LORs that terminate outside of the axial FOV of the bed position do not contribute to the sensitivity s_i. For the extreme edge slices, only LORs that are in the plane of the slice contribute to s_i. This

means that the penalty $P \propto 1/\gamma = 1/\sqrt{\lambda_i s_i}$ becomes large at the outer slices, leading to excessive noise suppression in the overlap regions and enhance potential for suppression of clinically relevant image features such as small tumors. The subsequent knitting together of adjacent bed position images at the overlap cannot recover these suppressed features, since both overlap regions will have this same "edge effect" in the penalty leading to loss of features. The alternative formulation in which s_i is replaced by the total counts in a local neighborhood is similarly affected since counts are not acquired for LORs that terminate outside the truncated axial FOV of the bed position.

[0024] In some disclosed embodiments, the local penalty in the overlap regions is reduced in order to account for the above effect.

[0025] In some embodiments disclosed herein, the reduction is proportional to the effective sensitivity increase (or effective total neighborhood counts increase) that would be achieved if the truncated volume k was continued into the adjacent overlapping truncated volume $k+1$. In one approach employing geometric sensitivity for adjusting the penalty, this amounts to replacing $\gamma_{i,k}^{sep} = \sqrt{\lambda_{i,k} s_{i,k}}$ with $\gamma_{i,k}^{joint} = \sqrt{\lambda_{i,k}(s_{i,k} + s_{i,k+1})}$ in the overlap region, where the $s_{i,k+1}$ term accounts for those LORs that are not part of the volume k (and hence do not contribute to geometric sensitivity $s_{i,k}$) but are part of the overlapping volume $k+1$ (and hence contribute to the geometric sensitivity $s_{i,k+1}$). A similar formulation can be used if locally adjusting γ using the total counts in a local neighborhood, by employing a summation of the total counts in the neighborhood of voxel i from both overlapping volumes k and $k+1$.

[0026] In the above embodiment, each volume k is still reconstructed separately. In an alternative joint reconstruction embodiment, the PET counts from all volumes is first combined and then reconstructed together. In this case $\gamma_{i,k}^{joint}$ is again used. Here a suitable formulation could be $\gamma_i^{joint} = \sqrt{\lambda_i(s_{i,k} + s_{i,k+1})}$ where λ_i is the value of voxel i produced by the (single) joint reconstruction of the combined data set.

[0027] In a variant embodiment, if acquisition times for the various bed positions are different then the sensitivities $s_{i,k}$ and $s_{i,k+1}$ are scaled proportionally to the acquisition times. This is due to a lower acquisition time resulting in fewer counts being acquired and correspondingly lower sensitivity. So, if the acquisition times are T_k and T_{k+1} for respective overlapping bed positions k and $k+1$ then the scaling is $s_{i,k} \rightarrow \frac{T_k \cdot s_{i,k}}{(T_k+T_{k+1})/2}$ and $s_{i,k+1} \rightarrow \frac{T_{k+1} \cdot s_{i,k+1}}{(T_k+T_{k+1})/2}$.

[0028] In other embodiments disclosed herein, an analogous approach can be applied to motion compensated PET imaging using (e.g. respiratory) gating. In this case, two successive gate phases ϕ_k and ϕ_{k+1} are considered, with some motion represented by a motion vector Δr occurring between the two phases. Then a possible formulation of the adjusted edge preservation parameter is $\gamma_{i,k}^{joint} = \sqrt{\lambda_{i,k}(s_i + s_{i+\Delta r})}$.

[0029] With reference to FIGURE 1, an illustrative medical imaging system **10** is shown. As shown in FIGURE 1, the system **10** includes an imaging or image acquisition device **12**. In one example, the image acquisition device **12** can comprise a PET imaging device including a PET gantry **13** and an array of radiation detectors **14** (diagrammatically indicated in FIGURE 1; typically, the radiation detectors of the PET gantry are arranged as a series of PET detector rings arranged to span an axial FOV). The illustrative image acquisition device **12** is a PET/CT scanner that further includes a computed tomography (CT) gantry **15**. A patient table (or bed) **16** is arranged to load a patient into an examination region **17** of the imaging device **12**, e.g. into the bore of the CT gantry **15** or into the bore of the PET gantry **13**. Commonly, the CT gantry **15** is used to acquire a CT image of the subject that is converted to an attenuation map of the subject. The PET gantry **13** acquires the PET imaging data which is reconstructed using the attenuation map from the CT image to account for radiation absorption in the patient in the PET image reconstruction.

[0030] The system **10** also includes a computer or workstation or other electronic data processing device **18** with typical components, such as at least one electronic processor **20**, at least one user input device (e.g., a mouse, a keyboard, a trackball, trackpad, and/or the like) **22**, and a display device **24** (for example, an LCD display, OLED display, plasma display, or the like). In some embodiments, the display device **24** can be a separate component from the computer **18**, and/or may comprise two or more displays. The workstation **18** can also include one or more databases or non-transitory storage media **26** (such as a magnetic disk, RAID, or other magnetic storage medium; a solid state drive, flash drive, electronically erasable read-only memory (EEROM) or other electronic memory; an optical disk or other optical storage; various combinations thereof; or so forth). The display device **24** is configured to display images acquired by the imaging system **10** and typically also to display a graphical user interface (GUI) **28** including various user dialogs, e.g. each with one or more fields, radial selection buttons, et cetera to receive a user input from the user input device **22**.

[0031] The at least one electronic processor **20** is operatively connected with the one or more databases **26** which stores instructions which are readable and executable by the at least one electronic processor **20** to perform disclosed operations including performing an

imaging method or process **100**. In some examples, the imaging method or process **100** may be performed at least in part by cloud processing.

[0032] With reference to FIGURE 2, an illustrative embodiment of the imaging method **100** is diagrammatically shown as a flowchart. At **102**, the at least one electronic processor **20** is programmed to receive, other otherwise operate or control the CT/PET imaging device **12** (and more particularly the PET gantry **13**) to, acquire PET imaging data on a frame by frame basis for frames along an axial direction with neighboring frames overlapping along the axial direction wherein the frames include at least a volume (k) and a succeeding volume (k+1) at least partially overlapping the volume (k) along the axial direction. At **104**, the at least one electronic processor **20** is programmed to generate an image of the volume (k) using an iterative image reconstruction process includes operations **106** and **108**. At **106**, a local penalty function is computed for suppressing noise over the volume (k) including reducing the value of the local penalty function in an overlap region. At **108**, an update image of the volume (k) is generated using imaging data from the volume (k) and further using the local penalty function. Although not illustrated, it will be understood that the iterative image reconstruction **104** may take into account radiation absorption in the subject using an attenuation map generated from a CT image acquired of the subject using the CT gantry **15**.

[0033] In one embodiment disclosed herein, the local penalty function depends on local geometric sensitivity of the PET imaging device **12** and the value of the local penalty function is reduced in the overlap region by an amount compensating for loss of geometric sensitivity due to axial truncation of the volume (k). An illustrative example is described next, in which the edge-preserving penalty function is a Relative Difference Prior (RDP) and ordered subset expectation maximization (OSEM) reconstruction is used. The update image indexed $n+1$ for iteration n is suitably written as:

$$\lambda_i^{n+1} = \lambda_i^n + \underbrace{\frac{\lambda_i^n}{s_{i,k}} \frac{\partial}{\partial \lambda_i} \left[\sum_{j=1}^{N} \left(y_i \log \left(\sum_{j'=1}^{p} a_{jj'} \lambda_i^n + r_j \right) - \left(\sum_{j'=1}^{p} a_{jj'} \lambda_i^n + r_j \right) \right) \right]}_{\text{MLE}} - \underbrace{\frac{\lambda_i^n}{s_{i,k}} \frac{\partial}{\partial \lambda_i} \left[\sum_{m \in N_i} \beta_{mi}^* \frac{(\lambda_i - \lambda_m)^2}{\lambda_i + \lambda_m + \gamma_i |\lambda_i - \lambda_m|} \right]}_{\text{local RDP penalty}} \quad (1)$$

where λ_i is the estimated activity at the voxel indexed by i, and $\beta_{mi}^{*} = \frac{w_m \beta_i}{\sum_{\forall m} w_m}$ is a local penalty weighting factor, a_{jj}, is the system matrix value, , $s_{i,k}$ is the geometric sensitivity at voxel i (preferably scaled by the acquisition time if different bed positions have different acquisition times), y_j is a data projection bin, and parameter $\gamma_i > 0$ is the edge preservation parameter and steers the RDP prior. The prior is estimated over local image neighborhood N_i around the voxel i. In general, a larger value of γ_i produces greater edge preservation (i.e., reduces the penalty). The value $\gamma_i = 0$ would eliminate edge preservation entirely, and the RDP becomes a quadratic prior.

[0034] As disclosed herein, the value of the local penalty function is reduced in the overlap region where bed positions of volumes k and $k+1$ overlap (and also where bed positions of volumes $k-1$ and k overlap, if current bed position k is overlapped on both ends). In some suitable embodiments, the local penalty function depends on the local geometric sensitivity $s_{i,k}$ of the PET imaging device **12** for the voxel indexed by i in the image volume of the bed position of volume k. The geometric sensitivity at a voxel i can be viewed as the number of lines of response (LORs) passing through that voxel i. In the portion of volume k that does not overlap either of the neighboring volumes $k-1$ or $k+1$, the standard sensitivity can be used, and for the n-th iteration the value $\gamma_i = \gamma_0 \sqrt{\lambda_{i,k}^{n} \cdot s_{i,k}}$ can be used, where γ_0 is a constant. However, in the overlap region the penalty is reduced. This is achieved by increasing the value of the edge preservation parameter γ in the overlap region by an amount compensating for loss of geometric sensitivity due to axial truncation of the volume k. Thus, a "joint" edge preservation parameter $\gamma_{i,k}^{joint}$ is used, which can be suitably written as $\gamma_{i,k}^{joint} = \gamma_0 \sqrt{\lambda_{i,k}^{n} \cdot \left(s_{i,k} + s_{i,k+1}\right)}$ where $s_{i,k+1}$ is the geometric sensitivity for the (same) voxel i in the next-neighboring volume $k+1$. Again, it is emphasized that this adjustment increases the edge preservation parameter (that is, $\lambda_{i,k}^{joint} > \lambda_{i,k}$) which, due to γ being in the denominator of the local RDP penalty of Equation (1), results in a reduction of the local RDP penalty in the overlap region. This reduction in the RDP penalty accounts for the additional data in volume $k+1$ which means that the noise is lower when the two reconstructed volumes k and $k+1$ are knitted together in the overlap region, so that a lower penalty can be employed in the overlap region when reconstructing the volume k to achieve a desired noise reduction, and hence the features (edges) are better preserved due to the reduced penalty in the overlap region.

[0035] In another embodiment, the local penalty function depends on the total coincidence counts passing through the voxel being penalized, and the value of the local penalty function is reduced in the overlap region by an amount compensating for the total coincidence counts passing through the voxel being penalized in the succeeding volume $k+1$. The penalty may be formulated in terms of actual local coincidence count statistics, rather than in terms of the geometric sensitivity. This entails replacing the geometric sensitivity s in the above expressions with actual counts. In this case, $\gamma_i = \gamma_0\sqrt{\lambda_{i,k}^n \cdot C_{i,k}}$ (without overlap adjustment) where $C_{i,k}$ is the count of coincidence events in the dataset for bed position k whose LORs pass through the voxel i. For time-of-flight (TOF) PET, this could be formulated as $\gamma_i = \gamma_0\sqrt{\lambda_{i,k}^n \cdot \sum_{v=1}^{C_{i,k}} w_v}$ where the index v runs over the $C_{i,k}$ coincidence counts of the dataset for bed position k whose LORs pass through the voxel i, and w_v is the time-of-flight probability that the count indexed by v originated in the voxel i. For the non-TOF case, the joint edge preservation parameter (i.e., providing for overlap adjustment) is $\gamma_{i,k}^{joint} = \gamma_0\sqrt{\lambda_{i,k}^n \cdot \left(C_{i,k} + C_{i,k+1}\right)}$ where again analogously the term $C_{i,k+1}$ is the count of coincidence events in the dataset for bed position $k+1$ whose LORs pass through the (same) voxel i. In this formulation it is even more explicit that the reduced penalty (which again is provided by an increased value of the denominator term $\gamma_{i,k}^{joint}$) accounts for the additional data $C_{i,k+1}$ in volume $k+1$ which means that the noise is lower when the two reconstructed volumes k and $k+1$ are knitted together in the overlap region. The equivalent formulation for TOF is $\gamma_{i,k}^{joint} = \gamma_0\sqrt{\lambda_{i,k}^n \cdot \left(\sum_{v=1}^{C_{i,k}} w_v + \sum_{v=1}^{C_{i,k+1}} w_v\right)}$ where the summation $\sum_{v=1}^{C_{i,k+1}} w_v$ is in the dataset for volume $k+1$.

[0036] In the above examples, the reconstruction process **106, 108** includes reconstructing each volume (k) of the imaging data separately from the other volumes (k) of the imaging data into a reconstructed bed position image, and then knitting the bed position images together in image space to generate the final image. In other embodiments, the reconstruction process **106, 108** can include combining the number of counts from all volumes (k) in the imaging data into a total volume; and reconstructing the total volume into a reconstructed image. In this latter embodiment, the local penalty function depends upon

$$\gamma_i^{joint} = \gamma_0\sqrt{\lambda_i^n \cdot \left(s_{i,k} + s_{i,k+1}\right)}$$

[0037] In either embodiment, if the acquisition times for successive bed positions are not all the same, then the reduction of the value of the local penalty function in the overlap region is suitably also scaled based on a ratio of respective acquisition times for the volume (k) and the succeeding volume $k + 1$.

[0038] With reference to FIGURE 3, an illustrative embodiment of a respiratory-gated imaging method **200** is diagrammatically shown as a flowchart. This is a different application, but the disclosed approach of adjusting the penalty in the (now temporal, rather than spatial/axial) overlap region is analogous. At **202**, the at least one electronic processor **20** is programmed to operate or control the PET imaging device **12** to acquire imaging data of a respiring patient. Concurrently with the PET imaging data acquisition, a respiratory gating signal is acquired by a respiration monitor **201** which provides respiratory phase-versus-time information. For example, the respiratory gating signal can be provided by the respiration monitor **201** comprising a respiration monitor belt that measures expansion and contraction of the chest during breathing; or the respiratory gating signal can be provided by the respiration monitor **201** comprising a flow sensor that measures air flow into/out of the mouth and/or nose; or so forth. At **203**, the PET data are binned by respiratory phase using the respiratory gating signal. By analogy to the multi-bed position imaging example of FIGURE 2, each respiratory phase bin is denoted by index k, and two adjacent respiratory phase bins k and k+1 are adjacent in the respiratory sequence, that is, in each breath interval the respiratory phase k+1 immediately follows the respiratory phase k in time. It will be appreciated that the binning by respiratory phase will result in the PET data acquired over the same respiratory phase k in successive breaths being combined to form the PET data set for respiratory phase bin k; and likewise the PET data acquired over the same respiratory phase k+1 in successive breaths will be combined to form the PET data set for respiratory phase bin k+1; and so forth. Moreover, the bins overlap in time. At **204**, the at least one electronic processor **20** is programmed to generating an image of the respiratory phase (k) using an iterative image reconstruction process operating on the acquired PET imaging data that is accumulated in the respiratory phase bin (k) over multiple breaths. The iterative reconstruction **204** includes operations **206**, **208,** and **210**. At **206**, the imaging data of each bin is adjusted for respiratory motion detected in the gate phases. This entails shifting the counts of LOR endpoints according to derived motion vectors. For each voxel i, there is an associated motion vector Δr_i indicating the movement of the voxel i from its reference position (which may, for example, be designated arbitrarily as its position at bin k=0 so that $\Delta r_{i,k=0}=0$ for all i). At **208**, a local penalty function is computed for suppressing noise in the respiratory phase bin (k) including reducing the value of the local

penalty function in a temporal overlap region with the respiratory phase bin k+1. At **210**, an update image of the respiratory phase bin (k) is generated using imaging data from the respiratory phase bin (k) and further using the local penalty function.

[0039] In some embodiments, the adjusting at operation **206** is performed according to:

$$\gamma_{i,k}^{joint} = \gamma_0 \sqrt{f_{i,k}(s_i + s_{i+\Delta r})}..$$

where γ is an edge preservation parameter, i is a voxel, λ is a greyscale value of the voxel, s is a geometric sensitivity passing through the voxel, and Δr is a motion vector between two gate phases ϕ_k and ϕ_{k+1}.

[0040] FIGURE 4 shows examples of reconstructed images using uniform phantom with six 6 mm diameter spheres in hexagonal pattern located in the center of the overlap region. The figure labeled (a) is an image reconstructed with a standard penalized reconstruction after knitting. The figure labeled (b) is an image reconstructed with a joint penalized reconstruction of the imaging method **100**. A side view of the phantom setup is shown in the figure labeled (c). A cylinder phantom **50** is shown with multiple spheres **52** over a first bed position **54** and second bed position **56.**

[0041] The disclosure has been described with reference to the preferred embodiments. Modifications and alterations may occur to others upon reading and understanding the preceding detailed description. It is intended that the disclosure be construed as including all such modifications and alterations insofar as they come within the scope of the appended claims or the equivalents thereof.

CLAIMS:

1. A non-transitory computer-readable medium storing instructions readable and executable by a workstation (**18**) including at least one electronic processor (**20**) to perform an imaging method (**100**), the method comprising:

receiving imaging data on a frame by frame basis for frames along an axial direction with neighboring frames overlapping along the axial direction wherein the frames include at least a volume (k) and a succeeding volume (k+1) at least partially overlapping the volume (k) along the axial direction; and

generating an image of the volume (k) using an iterative image reconstruction process in which an iteration of the iterative image reconstruction process includes:

computing a local penalty function for suppressing noise over the volume (k) including reducing the value of the local penalty function in an overlap region;

generating an update image of the volume (k) using imaging data from the volume (k) and further using the local penalty function.

2. The non-transitory computer-readable medium of claim 1, wherein the local penalty function depends on local geometric sensitivity of the PET imaging device (**12**) and the value of the local penalty function is reduced in the overlap region by an amount compensating for loss of geometric sensitivity due to axial truncation of the volume (k).

3. The non-transitory computer-readable medium of claim 2, wherein the local penalty function depends upon $\gamma_i^{joint} = \sqrt{\lambda_{i,k}^n \cdot \left(s_{i,k} + s_{i,k+1}\right)}$

where γ is an edge preservation parameter of the local penalty function, i indexes a voxel, $\lambda_{i,k}^n$ is the value of the voxel i in the iterative reconstruction of the volume k specifically in the update image n of that iterative reconstruction n, $s_{i,k}$ is the geometric sensitivity of the PET imaging device (**12**) for voxel i when acquiring data on the volume k and $s_{i,k+1}$ is the geometric sensitivity of the PET imaging device (**12**) for voxel i when acquiring data on the volume $k+1$.

4. The non-transitory computer-readable medium of claim 1, wherein the local penalty function depends on the total coincidence counts passing through the voxel being penalized, and the value of the local penalty function is reduced in the overlap region by an amount compensating for the total coincidence counts passing through the voxel being penalized in the succeeding volume $k + 1$.

5. The non-transitory computer-readable medium of claim 4, wherein the penalty function depends upon $\gamma_i = \sqrt{\lambda_{i,k}^n \cdot C_{i,k}}$

where γ is an edge preservation parameter of the local penalty function, i indexes a voxel, $\lambda_{i,k}^n$ is the value of the voxel i in the iterative reconstruction of the volume k specifically in the update image n of that iterative reconstruction n; $C_{i,k}$ is the count of coincidence events in the dataset for bed position of volume k whose LORs pass through the voxel i.

6. The non-transitory computer-readable medium of claim 5, wherein the PET imaging device (**12**) is a time-of-flight imaging device, and

the penalty function depends upon $\gamma_i = \sqrt{\lambda_{i,k}^n \cdot \sum_{v=1}^{C_{i,k}} w_v}$ where γ is an edge preservation parameter of the local penalty function, i indexes a voxel, $\lambda_{i,k}^n$ is the value of the voxel i in the iterative reconstruction of the volume k specifically in the update image n of that iterative reconstruction n; $C_{i,k}$ is the count of coincidence events in the dataset for bed position of volume k whose LORs pass through the voxel i; andthe index v runs over the $C_{i,k}$ coincidence counts of the dataset for bed position k whose LORs pass through the voxel i, and w_v is the time-of-flight probability that the count indexed by v originated in the voxel i.

7. The non-transitory computer-readable medium of any one of claims 1-6, wherein the reconstructing includes:

reconstructing the volume (k) of the imaging data separately from the other volumes (k) of the imaging data into a reconstructed image.

8. The non-transitory computer-readable medium of any one of claims 1-6, wherein the reconstructing includes:

combining the number of counts from the volumes (k) in the imaging data into a total volume; and

reconstructing the total volume into a reconstructed image.

9. The non-transitory computer-readable medium of claim 8, wherein the local penalty function depends upon $\gamma_i^{joint} = \sqrt{\lambda_{i,k}^n \cdot \left(s_{i,k} + s_{i,k+1}\right)}$

where γ is an edge preservation parameter of the local penalty function, i indexes a voxel, $\lambda_{i,k}^n$ is the value of the voxel i in the iterative reconstruction of the volume k specifically in the update image n of that iterative reconstruction n, $s_{i,k}$ is the geometric sensitivity of the PET imaging device (**12**) for voxel i when acquiring data on the volume k and $s_{i,k+1}$ is the geometric sensitivity of the PET imaging device (**12**) for voxel i when acquiring data on the volume $k + 1$.

10. The non-transitory computer-readable medium of any one of claims 1-8, wherein the reduction of the value of the local penalty function in the overlap region is scaled based on a ratio of respective acquisition times for the volume (k) and the succeeding volume $k + 1$.

11. An imaging system (**10**), comprising:

a positron emission tomography (PET) imaging device (**12**); and

at least one electronic processor (**20**) programmed to:

receive imaging data on a frame by frame basis for frames along an axial direction with neighboring frames overlapping along the axial direction wherein the frames include at least a volume (k) and a succeeding volume (k+1) at least partially overlapping the volume (k) along the axial direction; and

generate an image of the volume (k) using an iterative image reconstruction process in which an iteration of the iterative image reconstruction process includes:

computing a local penalty function for suppressing noise over the volume (k) including reducing the value of the local penalty function in an overlap region, the local penalty function depending on the total coincidence counts passing through the voxel being penalized, and the value of the local penalty function is reduced in the overlap region by an amount compensating for the total coincidence counts passing through the voxel being penalized in the succeeding volume $k + 1$;

generating an update image of the volume (k) using imaging data from the volume (k) and further using the local penalty function;

wherein the reconstructing includes:

combining the number of counts from the volumes (k) in the imaging data into a total volume; and

reconstructing the total volume into a reconstructed image.

12. The system (**10**) of claim 11, wherein the penalty function depends upon $\gamma_i = \sqrt{\lambda_{i,k}^n \cdot C_{i,k}}$

where γ is an edge preservation parameter of the local penalty function, i indexes a voxel, $\lambda_{i,k}^n$ is the value of the voxel i in the iterative reconstruction of the volume k specifically in the update image n of that iterative reconstruction n; $C_{i,k}$ is the count of coincidence events in the dataset for bed position of volume k whose LORs pass through the voxel i.

13. The system (**10**) of claim 12, wherein the PET imaging device (**12**) is a time-of-flight imaging device, and

the penalty function depends upon $\gamma_i = \sqrt{\lambda_{i,k}^n \cdot \sum_{v=1}^{C_{i,k}} w_v}$ where γ is an edge preservation parameter of the local penalty function, i indexes a voxel, $\lambda_{i,k}^n$ is the value of the voxel i in the iterative reconstruction of the volume k specifically in the update image n of that iterative reconstruction n; $C_{i,k}$ is the count of coincidence events in the dataset for bed position of volume k whose LORs pass through the voxel i; andthe index v runs over the $C_{i,k}$ coincidence counts of the dataset for bed position k whose LORs pass through the voxel i, and w_v is the time-of-flight probability that the count indexed by v originated in the voxel i.

14. The system (**10**) of claim 11, wherein the local penalty function depends upon $\gamma_i^{joint} = \sqrt{\lambda_{i,k}^n \cdot (s_{i,k} + s_{i,k+1})}$

where γ is an edge preservation parameter of the local penalty function, i indexes a voxel, $\lambda_{i,k}^n$ is the value of the voxel i in the iterative reconstruction of the volume k specifically in the update image n of that iterative reconstruction n, $s_{i,k}$ is the geometric sensitivity of the PET imaging device (**12**) for voxel i when acquiring data on the volume k and $s_{i,k+1}$ is the

geometric sensitivity of the PET imaging device (**12**) for voxel i when acquiring data on the volume $k+1$.

15. The system (**10**) of any one of claims 11-14, wherein the reduction of the value of the local penalty function in the overlap region is scaled based on a ratio of respective acquisition times for the volume (k) and the succeeding volume $k+1$.

16. An imaging method (**100**) performed on imaging data on a frame by frame basis for frames along an axial direction with neighboring frames overlapping along the axial direction wherein the frames include at least a volume (k) and a succeeding volume (k+1) at least partially overlapping the volume (k) along the axial direction, the method comprising:

generating an image of the volume (k) using an iterative image reconstruction process in which an iteration of the iterative image reconstruction process includes:

computing a local penalty function for suppressing noise over the volume (k) including reducing the value of the local penalty function in an overlap region, the local penalty function depends on local geometric sensitivity of the PET imaging device and the value of the local penalty function is reduced in the overlap region by an amount compensating for loss of geometric sensitivity due to axial truncation of the volume (k);

generating an update image of the volume (k) using imaging data from the volume (k) and further using the local penalty function;

wherein the reconstructing includes:

reconstructing the volume (k) of the imaging data separately from the other volumes (k) of the imaging data into a reconstructed image.

17. The imaging method (**100**) of claim 16, wherein the local penalty function depends upon $\gamma_i^{joint} = \sqrt{\lambda_{i,k}^n \cdot \left(s_{i,k} + s_{i,k+1}\right)}$

where γ is an edge preservation parameter of the local penalty function, i indexes a voxel, $\lambda_{i,k}^n$ is the value of the voxel i in the iterative reconstruction of the volume k specifically in the update image n of that iterative reconstruction n, $s_{i,k}$ is the geometric sensitivity of the PET imaging device (**12**) for voxel i when acquiring data on the volume k and $s_{i,k+1}$ is the geometric sensitivity of the PET imaging device (**12**) for voxel i when acquiring data on the volume $k+1$.

18. The imaging method (**100**) of either one of claims 16 and 17, wherein the reduction of the value of the local penalty function in the overlap region is scaled based on a ratio of respective acquisition times for the volume (k) and the succeeding volume $k + 1$.

19. An imaging method (**200**) performed on imaging data on a frame by frame basis for frames along an axial direction with neighboring frames overlapping along the axial direction wherein the frames include at least a volume (k) and a succeeding volume (k+1) at least partially overlapping the volume (k) along the axial direction, the method comprising:

generating an image of the volume (k) using an iterative image reconstruction process in which an iteration of the iterative image reconstruction process includes:

adjusting the imaging data with respiratory gating using two or more gate phases and motion detected in the gate phases;

computing a local penalty function for suppressing noise over the volume (k) including reducing the value of the local penalty function in an overlap region;

generating an update image of the volume (k) using imaging data from the volume (k) and further using the local penalty function.

20. The method (**200**) of claim 19, wherein the adjusting is performed according to:

$$\gamma_{i,k}^{joint} = \sqrt{f_{i,k}(s_i + s_{i+\Delta r})}$$

where γ is an edge preservation parameter, i is a voxel, f is a greyscale value of the voxel, s is a geometric sensitivity passing through the voxel, and Δr is a motion vector between two gate phases ϕ_k and ϕ_{k+1}.

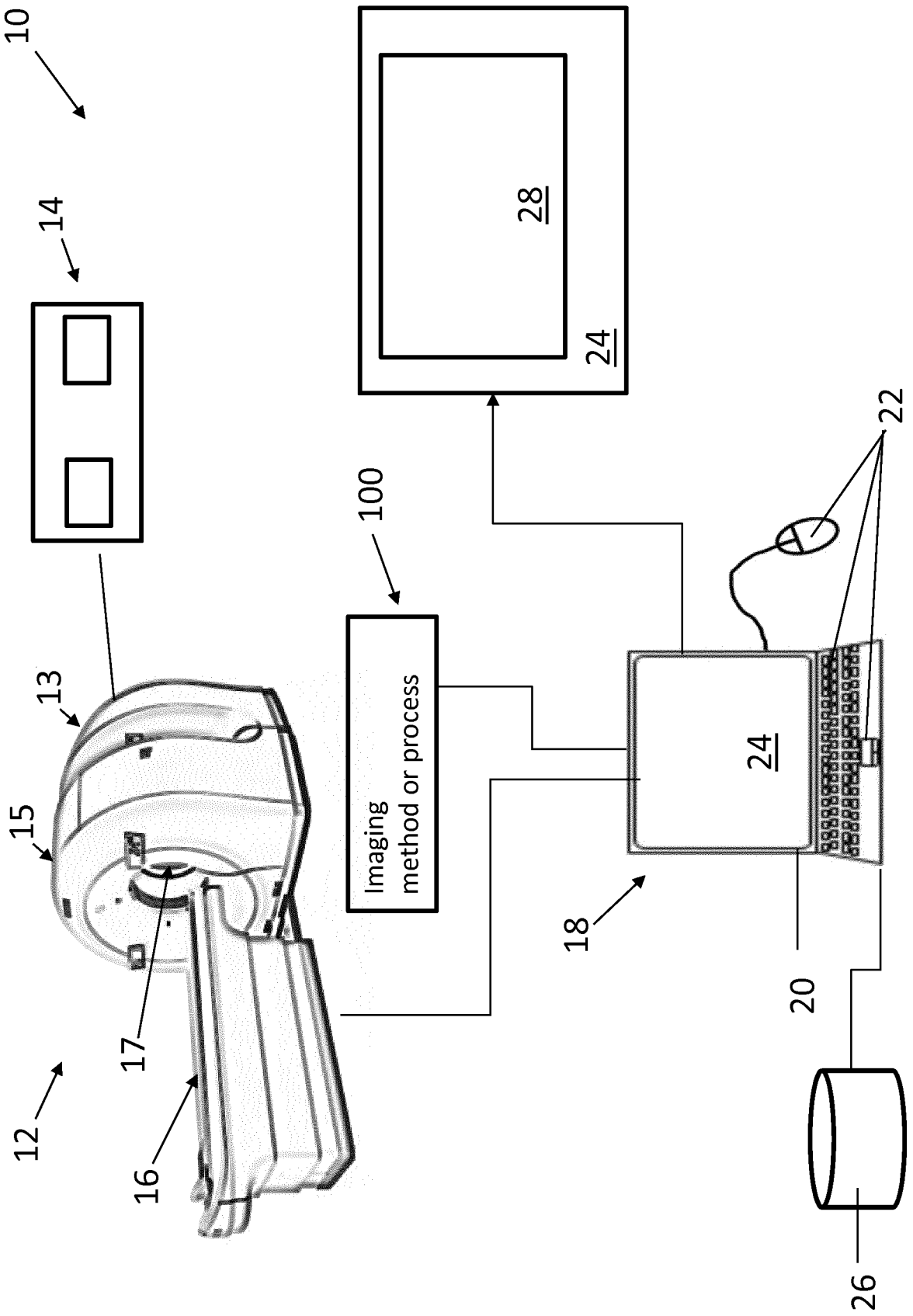
10
14
28
24
100
22
13
15
Imaging
method or process
24
18
17
20
12
16
26

Figure 1

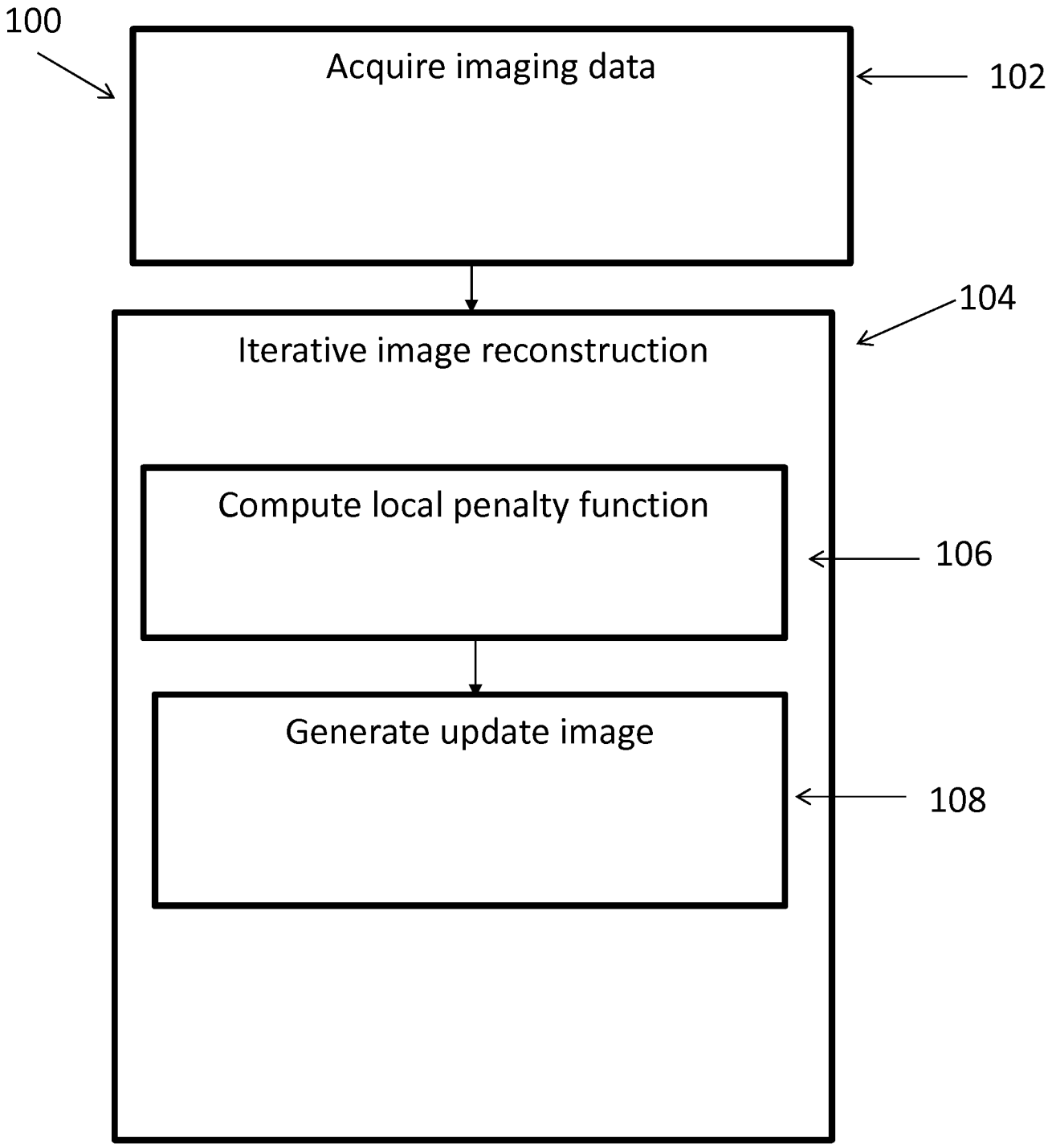
100
Acquire imaging data
102
104
Iterative image reconstruction
Compute local penalty function
106
Generate update image
108

Figure 2

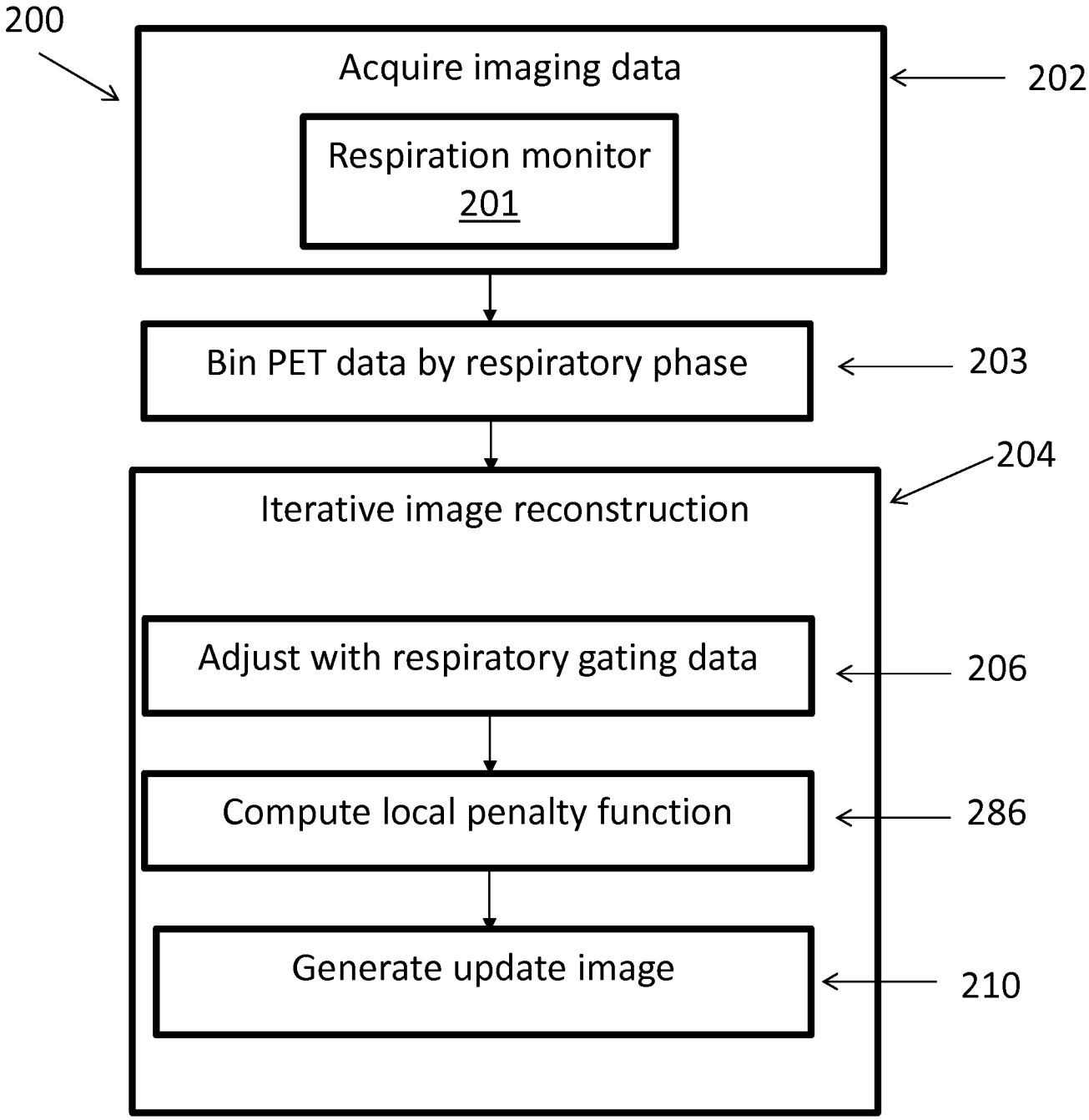
200
Acquire imaging data
Respiration monitor
201
202
Bin PET data by respiratory phase
203
204
Iterative image reconstruction
Adjust with respiratory gating data
206
Compute local penalty function
286
Generate update image
210

Figure 3

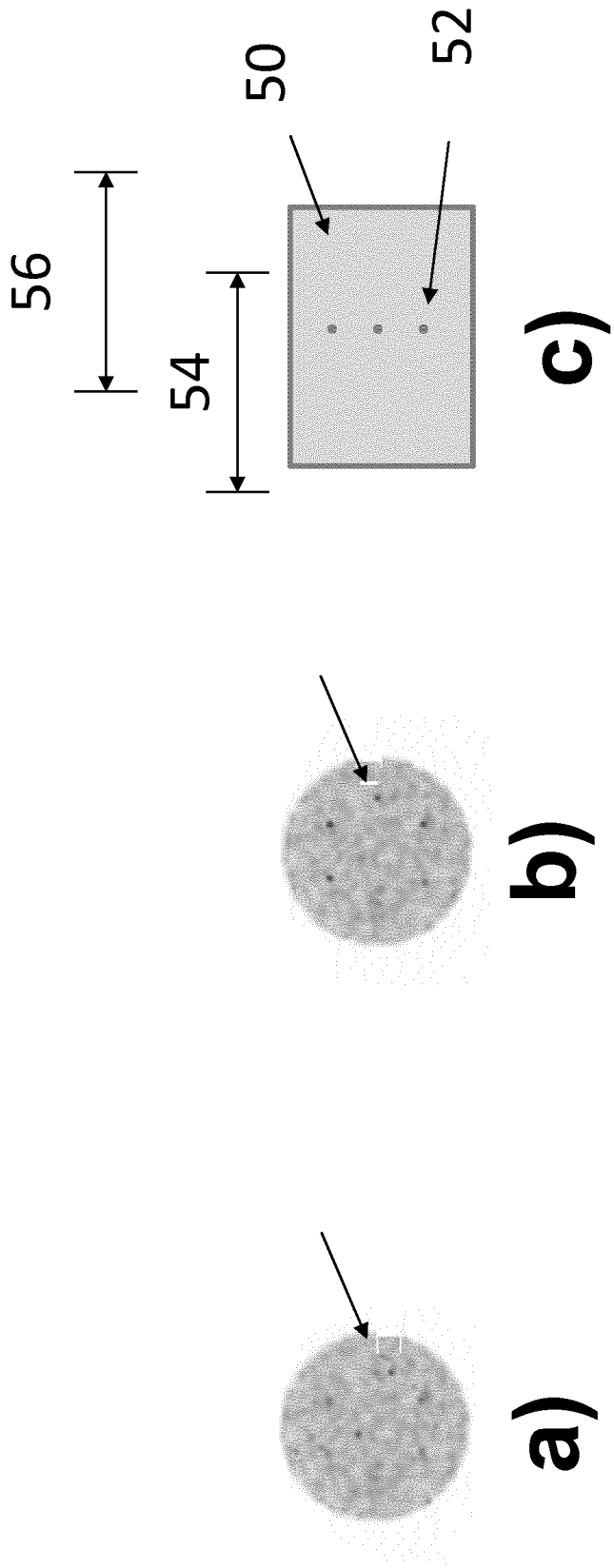

Figure 4

INTERNATIONAL SEARCH REPORT

International application No
PCT/EP2019/081515

A. CLASSIFICATION OF SUBJECT MATTER
INV. G06T11/00
ADD.

According to International Patent Classification (IPC) or to both national classification and IPC

B. FIELDS SEARCHED

Minimum documentation searched (classification system followed by classification symbols)
G06T

Documentation searched other than minimum documentation to the extent that such documents are included in the fields searched

Electronic data base consulted during the international search (name of data base and, where practicable, search terms used)

EPO-Internal, WPI Data, COMPENDEX, INSPEC

C. DOCUMENTS CONSIDERED TO BE RELEVANT

Category*	Citation of document, with indication, where appropriate, of the relevant passages	Relevant to claim No.
X	US 2017/103551 A1 (SUN ZHIPENG [CN] ET AL) 13 April 2017 (2017-04-13) cited in the application abstract figure 3 paragraph [0031] paragraph [0134] - paragraph [0151] paragraph [0176] - paragraph [0177] -----	1-20
X	US 2017/249758 A1 (MISTRETTA CHARLES A [US] ET AL) 31 August 2017 (2017-08-31) abstract paragraph [0054] -----	1,11,16, 19
	-/--	

[X] Further documents are listed in the continuation of Box C.

[X] See patent family annex.

* Special categories of cited documents :

"A" document defining the general state of the art which is not considered to be of particular relevance

"E" earlier application or patent but published on or after the international filing date

"L" document which may throw doubts on priority claim(s) or which is cited to establish the publication date of another citation or other special reason (as specified)

"O" document referring to an oral disclosure, use, exhibition or other means

"P" document published prior to the international filing date but later than the priority date claimed

"T" later document published after the international filing date or priority date and not in conflict with the application but cited to understand the principle or theory underlying the invention

"X" document of particular relevance; the claimed invention cannot be considered novel or cannot be considered to involve an inventive step when the document is taken alone

"Y" document of particular relevance; the claimed invention cannot be considered to involve an inventive step when the document is combined with one or more other such documents, such combination being obvious to a person skilled in the art

"&" document member of the same patent family

Date of the actual completion of the international search	Date of mailing of the international search report
15 January 2020	30/01/2020

Name and mailing address of the ISA/	Authorized officer
European Patent Office, P.B. 5818 Patentlaan 2 NL - 2280 HV Rijswijk Tel. (+31-70) 340-2040, Fax: (+31-70) 340-3016	Leclercq, Philippe

1

Form PCT/ISA/210 (second sheet) (April 2005)

INTERNATIONAL SEARCH REPORT

International application No
PCT/EP2019/081515

C(Continuation). DOCUMENTS CONSIDERED TO BE RELEVANT

Category*	Citation of document, with indication, where appropriate, of the relevant passages	Relevant to claim No.
X	US 2016/063741 A1 (YE HONGWEI [US] ET AL) 3 March 2016 (2016-03-03) abstract figure 9(A) and (B) figure 11 paragraph [0085] - paragraph [0087]	1,11,16, 19
X	US 2009/123048 A1 (LEROUX JEAN-DANIEL [CA] ET AL) 14 May 2009 (2009-05-14) abstract paragraph [0086]	1,11,16, 19
A	US 2017/061629 A1 (ZHU WENTAO [US] ET AL) 2 March 2017 (2017-03-02) the whole document	1-20

1

INTERNATIONAL SEARCH REPORT

Information on patent family members

International application No
PCT/EP2019/081515

Patent document cited in search report	Publication date	Patent family member(s)	Publication date
US 2017103551 A1	13-04-2017	CN 105389788 A	09-03-2016
		US 2017103551 A1	13-04-2017
US 2017249758 A1	31-08-2017	US 2017249758 A1	31-08-2017
		WO 2017147238 A1	31-08-2017
US 2016063741 A1	03-03-2016	JP 6556492 B2	07-08-2019
		JP 2016050932 A	11-04-2016
		US 2016063741 A1	03-03-2016
US 2009123048 A1	14-05-2009	CA 2631004 A1	09-11-2008
		US 2009123048 A1	14-05-2009
US 2017061629 A1	02-03-2017	EP 3226766 A1	11-10-2017
		US 2017061629 A1	02-03-2017
		US 2018374205 A1	27-12-2018
		WO 2017032297 A1	02-03-2017